Nonlinear Increase of Elongation Rate of Actin Filaments with Actin Monomer Concentration†

Thomas Keiser, Achim Schiller, and Albrecht Wegner*

Institute of Physiological Chemistry I, Ruhr-University, D-4630 Bochum, Federal Republic of Germany

Received January 24, 1986; Revised Manuscript Received April 22, 1986

ABSTRACT: The nonlinear increase of the elongation rate of actin filaments above the critical monomer concentration was investigated by nucleated polymerization of actin. Significant deviations from linearity were observed when actin was polymerized in the presence of magnesium ions. When magnesium ions were replaced by potassium or calcium ions, no deviations from linearity could be detected. The nonlinearity was analyzed by two simple assembly mechanisms. (i) In the first model, if the ATP hydrolysis by polymeric actin is approximately as fast as the incorporation of monomers into filaments, terminal subunits of lengthening filaments are expected to carry to some extent ADP. As ADP-containing subunits dissociate from the ends of actin filaments faster than ATP-containing subunits, the rate of elongation of actin filaments would be nonlinearly correlated with the monomer concentration. (ii) In the second model (conformational change model), actin monomers and filament subunits were assumed to occur in two conformations. The association and dissociation rates of actin molecules in the two conformations were thought to be different. The equilibrium distribution between the two conformations was assumed to be different for monomers and filament subunits. The ATP hydrolysis was thought to lag behind polymerization and conformational change. As under the experimental conditions the rate of ATP hydrolysis by polymeric actin was independent of the concentration of filament ends, the observed nonlinear increase of the rate of elongation with the monomer concentration above the critical monomer concentration was unlikely to be caused by ATP hydrolysis at the terminal subunits. The conformational change model turned out to be the simplest assembly mechanism by which all available experimental data could be explained.

The rate of actin polymerization has been found to increase linearly with the concentration of monomeric actin within a certain range of monomer concentrations (Pollard & Mooseker, 1981; Bonder et al., 1983). Deviations from this linear correlation have been reported to occur at the critical monomer concentration (Carlier et al., 1984). This deviation has been attributed to a lag of ATP hydrolysis after binding of actin monomers to filament ends [Carlier et al., 1984; Pollard & Weeds, 1984; for a review, see Wegner (1985)]. Above the critical monomer concentration where actin filaments elongate, the ends of actin filaments carry a string of subunits with bound ATP, referred to as an "ATP cap" (Pardee & Spudich, 1982; Brenner & Korn, 1983; Grazi et al., 1984). Below the critical monomer concentration where actin filaments shorten, filaments lose their ATP caps and have ADP-containing subunits at their ends. ADP-bearing subunits dissociate about 5 times as fast from filament ends as ATP-containing subunits (Pollard, 1984). It follows that the rate of shortening and of lengthening of filaments depends on the monomer concentration in a different way (Hill & Kirschner, 1982; Hill & Carlier, 1983).

Deviations from linearity above the critical monomer concentration were reported by Pantaloni et al. (1985a,b). This nonlinearity was explained by a model in which the two terminal subunits were thought to have no ATPase activity. ATP was assumed to be hydrolyzed at an interphase between ADP-containing subunits of the core of actin filaments and the terminal ATP-containing subunits.

In this paper we discuss possible reasons for the nonlinear correlation above the critical monomer concentration. First, we attempt to modify the concept of ATP caps of growing filaments. If the ATP hydrolysis by polymeric actin is approximately as fast as the incorporation of monomers into filaments, terminal subunits of growing filaments are expected to carry to some extent ADP (Pantaloni et al., 1985a). ATP hydrolysis would affect the rate of elongation of actin filaments. Second, we discuss the possibility that a conformational change of actin leads to the observed nonlinear behavior. Conformational changes of actin have been reported previously (Higashi & Oosawa, 1965; Rich & Estes, 1976; Rouayrenc & Travers, 1981). The conformations of polymeric and of monomeric actin have been found to be different (Higashi & Oosawa, 1965). The conformation of actin monomers has been reported to alter on exchange of a tightly bound calcium ion for a magnesium ion (Frieden, 1982; Cooper et al., 1983). This conformational change requires ATP bound to actin monomers (Frieden & Patane, 1985). We consider the possibility that the rate of elongation is nonlinearly correlated to the monomer concentration as a result of a conformational change.

Materials and Methods

Preparation of Actin. Actin was prepared according to the method of Rees and Young (1967). The protein was applied to a Sephacryl S-200 column (2.5 × 90 cm). Part of the protein was modified with *N*-ethylmaleimide at cysteine-374 and subsequently with 7-chloro-4-nitro-2,1,3-benzoxadiazole at lysine-373 to produce a fluorescently labeled actin (Detmers et al., 1981). The concentration of actin was determined photometrically at 290 nm with an extinction coefficient of 24 900 M^{-1} cm^{-1} (Wegner, 1976). Monomeric actin with

†Supported by the Deutsche Forschungsgemeinschaft (Sonderforschungsbereich 168). Essential parts of the M.D. Thesis by A.S. are included in this paper.

0006-2960/86/0425-4899$01.50/0

bound ϵ-ATP[1] (ϵ-ATP–actin) was prepared by applying actin to a Fractogel TSK HW-50(S) column (2.5 × 40 cm) equilibrated with a buffer containing 0.4 mM ϵ-ATP, 0.2 mM $CaCl_2$, 200 mg/L NaN_3, and 5 mM triethanolamine hydrochloride (pH 7.5) (Wanger & Wegner, 1983).

Preparation of ϵ-ATP. ϵ-ATP was prepared according to the method of Secrist et al. (1972) with the modification that the crude product was applied to a DEAE-Sephadex A-25 column (2.5 × 40 cm) and eluted with a linear NH_4HCO_3 gradient (0.15–0.33 M) (Wanger & Wegner, 1983). The ϵ-ATP was analyzed as described previously (Wanger & Wegner, 1983).

Fluorescence. Actin polymerization was followed by the 2.2–2.5-fold greater fluorescence intensity of polymeric actin compared to that of monomeric actin (Detmers et al., 1981). Five percent of fluorescently labeled actin was copolymerized with unmodified actin. This low proportion of labeled actin does not significantly alter the polymerization rate or extent of assembly of unmodified actin (Wegner, 1982). The fluorescence intensity was measured by using a Perkin-Elmer LS-3 fluorometer. The excitation wavelength was 436 nm, and the fluorescence intensity was measured at 530 nm. The fluorescence intensity of monomeric and polymeric actin was calibrated as described previously (Schröer & Wegner, 1985).

Phosphate Determination. The ATP hydrolysis by actin was stopped by the addition of 0.2 mL of trichloroacetic acid (1 g/mL) to 2-mL samples. The phosphate resulting from the ATP hydrolysis was determined by a procedure employing extraction of phosphomolybdic acid and reduction by stannous chloride (Martin & Doty, 1949). The original method was modified as described previously (Wegner & Neuhaus, 1981).

Experimental Procedure. Monomeric actin was dialyzed against a buffer containing 0.5 mM ATP or 0.4 mM ϵ-ATP, 10 μM $MgCl_2$, 200 mg/L NaN_3, 5 mM triethanolamine hydrochloride (pH 7.5), and 1 mM dithiothreitol. Polymers were formed by adjusting the magnesium concentration to 0.7 mM and the EGTA concentration to 0.5 mM. The actin concentration was 25 μM. The polymerization of monomers onto filaments was followed by a method described previously (Pollard, 1983). Briefly, buffer, magnesium, and EGTA were mixed in a fluorescence cell. Monomeric and polymeric actin and the fluorescence cell were incubated for 10 min at 20 °C. Monomers and polymers were pipetted into the fluorescence cell to give final concentrations of 0.7 mM $MgCl_2$ and 0.5 mM EGTA and the desired concentrations of monomeric (2–16 μM) and polymeric actin (1–5 μM). The cell was mounted in a 20 °C thermostated cell holder placed in the fluorescence spectrometer. The association of monomers with filament ends was measured by the increase of the fluorescence intensity. The fluorescence intensity was recorded in intervals of 1 min to avoid continuous illumination of the samples. In agreement with the results reported by Pollard (1983), the time courses of fluorescence intensity were surprisingly reproducible even when different samples of polymeric actin were used.

Results

Nucleated Polymerization of Actin. Pantaloni et al. (1985b) have shown that above the critical concentration the rate of elongation of actin filaments does not increase linearly with the monomer concentration. We confirm these results in this section. Various concentrations of polymeric and monomeric actin were mixed, and the incorporation of monomers into filaments was measured by the increase of the fluorescence intensity. Two experiments were performed to prove that in the course of the measurement no new filaments are formed by nucleation or fragmentation of filaments. Figure 1 shows a plot of four nucleated polymerization curves of ϵ-ATP–actin. In all four experiments the initial monomer concentration was 4 μM. The initial polymer subunit concentrations ranged from 1 to 4 μM. The polymerization curves were represented in a plot of the time multiplied by the initial polymer subunit concentration c_{fi} vs. the concentration of incorporated subunits. The curves were congruent in this graph. This suggests that no new filaments were formed in the course of the experiment as the concentration of filament ends c_p is proportional to the concentration of initially added subunits ($c_p \sim c_{fi}$).

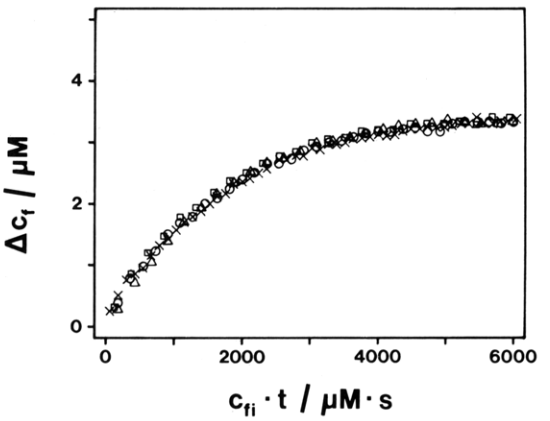

FIGURE 1: Time course of polymerization of 4 μM ϵ-ATP–actin nucleated by various concentrations of polymeric actin. Δc_f is the increase of the concentration of polymeric actin. Initial concentrations of polymeric actin c_{fi}: (×) 1, (□) 2, (○) 3, and (△) 4 μM. The curves were superimposed by plotting Δc_f vs. c_{fi} multiplied by time t.

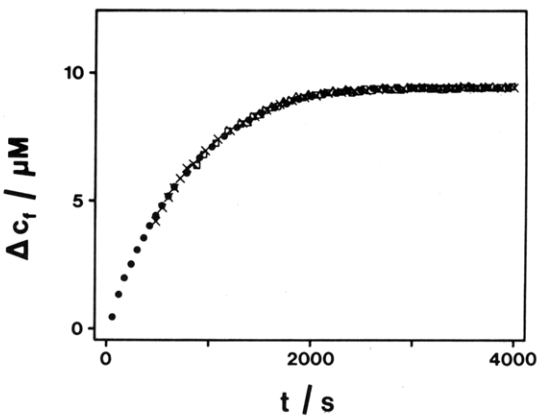

FIGURE 2: Time course of polymerization of various concentrations of ϵ-ATP–actin nucleated by 3 μM polymeric ϵ-ATP–actin. Δc_f is the increase of the concentration of polymeric actin. Initial concentrations of monomeric actin: (△) 2, (□) 4, (×) 6, and (●) 10 μM. The starting points were arranged so that an as good as possible superimposition of the curves was achieved.

Figures 2 and 3 show two other sets of polymerization curves. The initial polymer subunit concentration was kept constant, and the initially added monomer concentration was varied. A concentration of 2–10 μM monomeric ϵ-ATP–actin was polymerized onto 3 μM polymeric ϵ-ATP–actin (Figure 2), and 4–16 μM monomeric ATP–actin was combined with 4 μM polymeric ATP-actin (Figure 3). All four curves were superimposable if the starting points were appropriately arranged. The two tests were carried out at various monomer and polymer concentrations. The concentration of filament ends of ϵ-ATP–actin turned out to be constant if the initial polymer subunit concentration was equal to or above 1 μM

[1] Abbreviations: ϵ-ATP, 1,N^6-ethenoadenosine 5′-triphosphate; EGTA, ethylene glycol bis(β-aminoethyl ether)-*N,N,N′,N′*-tetraacetic acid.

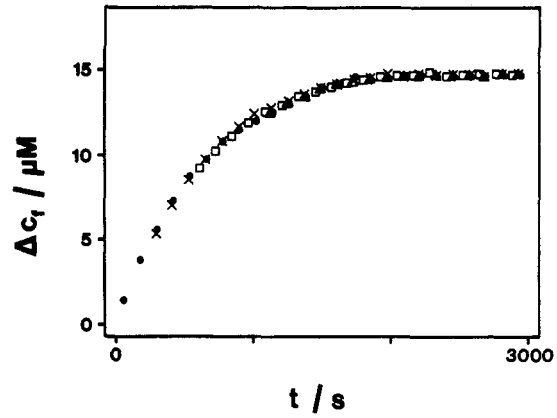

FIGURE 3: Time course of polymerization of various concentrations of ATP–actin nucleated by 4 μM polymeric ATP–actin. Δc_f is the increase of the concentration of polymeric actin. Initial concentrations of monomeric actin: (△) 4, (□) 8, (×) 12, and (●) 16 μM. The starting points were arranged so that an as good as possible superimposition of the curves was achieved.

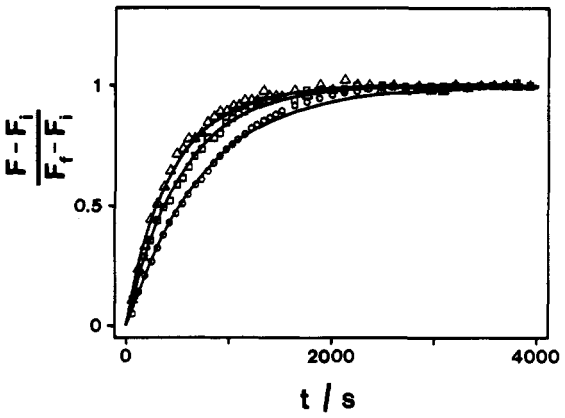

FIGURE 4: Time course of polymerization of various concentrations of ϵ-ATP–actin nucleated by 3 μM polymeric ϵ-ATP–actin. The polymerization is represented by the change of the fluorescence intensity normalized by the total change of the fluorescence intensity. F, fluorescence intensity; F_i, initial fluorescence intensity; F_f, final fluorescence intensity. Initial concentrations of monomeric actin: (△) 2, (□) 6, and (○) 10 μM. (—) Fitted exponential curves.

and the initial monomer concentration was below 5 μM. At 10 μM initial monomer concentration the concentration of filament ends was kept constant if the initial polymer subunit concentration was at least 2 μM.

Critical Monomer Concentration. At the final stage of polymerization, a constant monomer concentration is reached that is thought to be independent of the total actin concentration (Oosawa & Kasai, 1962). The critical monomer concentration under the conditions of this experiment was determined by extrapolation of a plot of the total actin concentration vs. the polymerized actin concentration toward zero polymerized actin concentration (Oosawa & Kasai, 1962; Wegner & Savko, 1982). The critical concentration of ϵ-ATP–actin scattered between 0.5 and 0.7 μM, and the average critical monomer concentration was 0.6 μM. The critical monomer concentration of ATP–actin was found to be 1.4 μM.

Nonexponential Nucleated Polymerization Curves. Figure 4 depicts nucleated polymerization curves of ϵ-ATP–actin. A concentration of 2, 6, or 10 μM monomeric ϵ-ATP–actin was polymerized onto 3 μM polymeric ϵ-ATP–actin. In Figure 4, the change of the fluorescence intensity normalized by the total change of the fluorescence intensity vs. time is plotted. Fitted exponential curves are depicted in Figure 4, too. The half-times of the three fitted exponential curves are different.

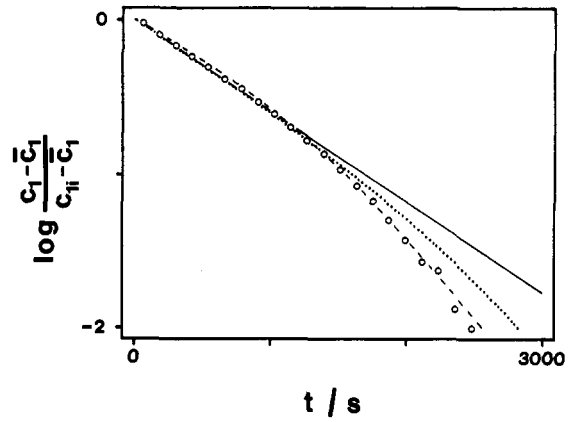

FIGURE 5: Logarithmic representation of time course of polymerization of 10 μM ϵ-ATP–actin nucleated by 3 μM polymeric ϵ-ATP–actin. c_1, monomer concentration; $\bar{c}_1$ = 0.6 μM, critical monomer concentration; c_{1i} = 10 μM, initial monomer concentration. (○) Experimental data. (—) Exponential fit (rate constant 0.00135 s^{-1}). (···) Fit of ATP hydrolysis model: $k^+ = 8 \times 10^6$ M^{-1} s^{-1}, $k_T^- = 1$ s^{-1}, $k_D^- = 20$ s^{-1}, $k_p = 2.5$ s^{-1}, and $c_p = 0.16$ nM. (– –) Fit of the conformational change model: $K_{con} = 3$, $k_{con}^+ = 0.5$ s^{-1}, $K'_{con} = 3$, $K_{gg} = 0.555 \times 10^6$ M^{-1}, $k_{gg}^- = 0.1$ s^{-1}, $k_{gp}^- = 2$ s^{-1}, $k_{pg}^- = 0.2$ s^{-1}, $k_{pp}^- = 3$ s^{-1}, and $c_p = 0.72$ nM.

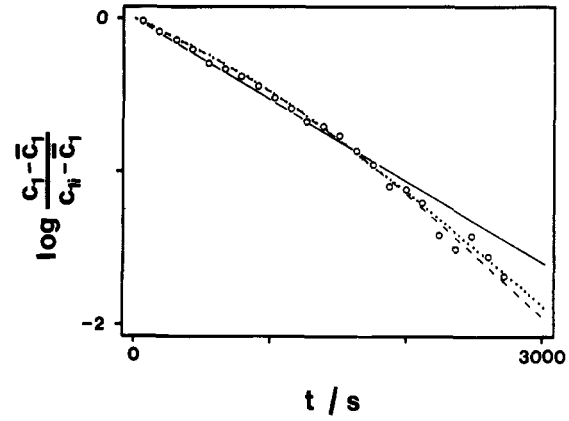

FIGURE 6: Logarithmic representation of time course of polymerization of 16 μM ATP–actin nucleated by 3 μM polymeric ATP–actin. c_1, monomer concentration; $\bar{c}_1$ = 1.4 μM, critical monomer concentration; c_{1i} = 16 μM, initial monomer concentration. (○) Experimental data. (—) Exponential fit (rate constant 0.0013 s^{-1}). (···) Fit of ATP hydrolysis model: $k^+ = 5 \times 10^6$ M^{-1} s^{-1}, $k_T^- = 1$ s^{-1}, $k_D^- = 20$ s^{-1}, $k_p = 5$ s^{-1}, and $c_p = 0.22$ nM. (– –) Fit of conformational change model: $K_{con} = 3$, $k_{con}^+ = 0.5$ s^{-1}, $K'_{con} = 3$, $K_{gg} = 0.238 \times 10^6$ M^{-1}, $k_{gg}^- = 0.1$ s^{-1}, $k_{gp}^- = 2$ s^{-1}, $k_{pg}^- = 0.2$ s^{-1}, $k_{pp}^- = 3$ s^{-1}, and $c_p = 1.32$ nM.

This observation cannot be explained by a most simple reaction mechanism in which actin monomers (concentration c_1) bind with a rate constant k^+ to a constant number of filament ends (concentration c_p) and filament subunits dissociate with a rate constant k^- from filament ends:

$$dc_1/dt = -k^+c_1c_p + k^-c_p = -k^+(c_1 - \bar{c}_1)c_p \quad (1)$$

or

$$c_1 - \bar{c}_1 = (c_{1i} - \bar{c}_1)e^{-k^+c_pt} \quad (2)$$

c_{1i} is the initial monomer concentration, and $\bar{c}_1$ is the critical monomer concentration at which monomers bind to the filament ends at the same rate ($k^+\bar{c}_1$) as filament subunits dissociate (k^-):

$$\bar{c}_1 = k^-/k^+ \quad (3)$$

If this most simple assembly mechanism applied to actin polymerization, the monomer concentration would be expected to decay exponentially with a half-time of $\ln 2/(k^+c_p)$ inde-

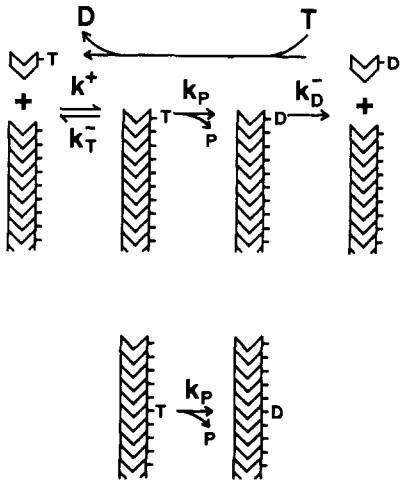

FIGURE 7: Reaction scheme of ATP hydrolysis model. Monomers and filament subunits are represented by chevrons. T, D, and P stand for ATP, ADP, and inorganic phosphate, respectively.

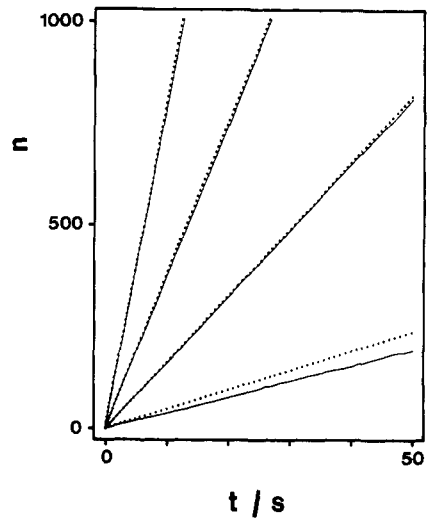

FIGURE 8: Monte Carlo calculation and steady-state approximation of ATP hydrolysis model: n, number of filament subunits; continuous lines, Monte Carlo calculations (50 times repeated and averaged); dotted lines, steady-state approximations. Monomer concentrations: 2, 4, 8, and 16 μM. $k^+ = 5 \times 10^6$ M^{-1} s^{-1}, $k_T^- = 1$ s^{-1}, $k_D^- = 20$ s^{-1}, and $k_p = 5$ s^{-1} (see Figure 6).

pendently of the initial monomer concentration. Figure 4 shows significant deviations from this behavior. Furthermore, the individual measured curves reveal systematic deviations from exponential curves. The measured curves reach the final critical monomer concentration faster than the fitted exponential curves (Figure 4, 10 μM initial monomer concentration). These deviations appear enlarged in a plot in which the concentration is represented logarithmically (Figures 5 and 6). The polymerization curves of ϵ-ATP–actin (Figure 5) deviate from exponential curves more strongly than ATP–actin (Figure 6). Therefore, mainly ϵ-ATP–actin was used for the analysis of polymerization. These deviations were observed when actin was polymerized in the presence of magnesium ions. When magnesium was replaced by potassium or calcium or by a combination of potassium and magnesium, no significant deviations could be detected. These results suggest that at least in the presence of magnesium ions actin polymerization cannot be described by a simple association–dissociation reaction that leads to a linear increase of the rate of elongation of actin filaments with the monomer concentration (Pantaloni et al., 1985b). In the following section, more complicated reaction mechanisms will be discussed.

Models of Linear Polymerization. The assumption that actin monomers bind to filament ends in a one-step reaction is probably a simplification (Cooke, 1975). More-step reactions may account for the observed nonexponential decay of the monomer concentration. Two-step assembly reactions will therefore be discussed in the following section, and the derived two-step polymerization models will be compared to the experimental data.

(*i*) *Reversible Assembly Reaction Followed by Irreversible ATP Hydrolysis.* A theory of the interference of nucleoside triphosphate hydrolysis in the mechanism of linear polymerization has been derived by Hill and Kirschner (1982), Hill and Carlier (1983), and Chen and Hill (1983). The theoretical treatment of ATP hydrolysis developed in this study is based on the method by Hill and Kirschner (1982). A modified reaction scheme is depicted in Figure 7. The terminal subunit of the filament can bind ATP or ADP. Monomeric ATP–actin can associate with a filament end independently of whether the terminal subunit of the filament binds ATP or ADP. The newly incorporated subunit can dissociate or it can hydrolyze ATP to yield a terminal subunit with bound ADP. A terminal ADP-containing subunit can dissociate, too. The actin monomer with bound ADP exchanges its nucleotide for ATP if present in excess over ADP (Seidel et al., 1966; Neidl & Engel, 1979; Wanger & Wegner, 1983). The monomeric ATP–actin may associate again.

The rate of elongation of filaments is given by (Figure 7)

$$dn/dt = k^+c_1 - k_T^-a_1 - k_D^-(1 - a_1) \qquad (4)$$

a_1 is the probability that the terminal subunit binds ATP. The rate constants are defined in Figure 7. The elongation rate does not increase linearly with the monomer concentration as the probability a_1 depends on the monomer concentration in complicated manner. At high monomer concentrations, the average time between two association reactions decreases, leaving less time for ATP hydrolysis between two association reactions. Thus, at high monomer concentrations the probability a_1 that the terminal subunit binds ATP is greater than at low monomer concentrations. If the actin monomer concentration is kept constant, a steady state will be reached in which the rate of monomer consumption and the rate of ATP hydrolysis are constant. The elongation rate and the rate of ATP hydrolysis can easily be calculated by solving the steady-state equations. The probability a_1 is given by the following steady-state equation (see Figure 7):

$$da_1/dt = 0 = k^+c_1(1 - a_1) - k_T^-a_1(1 - a_2) + k_D^-(1 - a_1)a_2 - k_Pa_1 \qquad (5)$$

where a_2 is the probability that the second subunit from the end binds ATP. The probability a_n that the nth subunit from the end ($n \geq 2$) contains bound ATP is given by (Figure 7)

$$da_n/dt = 0 = k^+c_1[a_{n-1}(1 - a_n) - (1 - a_{n-1})a_n] + k_T^-a_1[(1 - a_n)a_{n+1} - a_n(1 - a_{n+1})] + k_D^-(1 - a_1)[(1 - a_n)a_{n+1} - a_n(1 - a_{n+1})] - k_Pa_n \qquad (6)$$

The ratio of the probabilities a_{n+1} and a_n can be calculated to be

$$\frac{a_{n+1}}{a_n} = \frac{k^+c_1 - a_1(k_T^- + k_P)}{k^+c_1 - a_1k_T^-} \qquad n \geq 1 \qquad (7)$$

Combining eq 5 and 7 yields an equation that renders possible calculation of the probability a_1 in terms of the rate constants and of the monomer concentration c_1. The applicability of the steady-state approximation can be tested by Monte Carlo

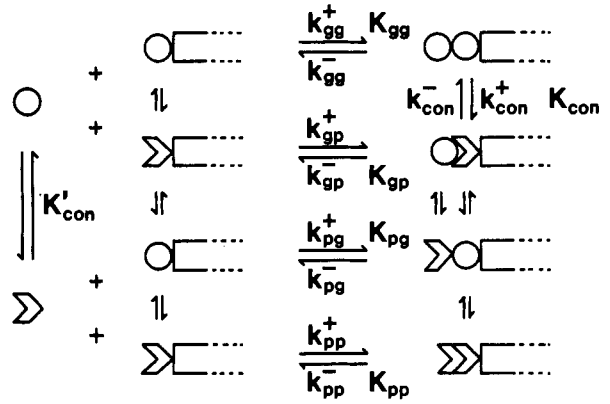

FIGURE 9: Reaction scheme of conformational change model. Actin molecules in the g conformation are represented by circles; actin molecules in the p conformation are represented by chevrons.

calculations. Figure 8 shows that the agreement of the steady-state approximation with Monte Carlo calculations is good for a set of rate constants that have been selected for the fit to the experimental data (see Fit of Models to Nucleated Polymerization Curves).

The time course of consumption or production of monomers at the filament ends can be calculated to be

$$dc_1/dt = (dn/dt)c_p = [k^+c_1 - k^-_T a_1 - k^-_D(1 - a_1)]c_p \quad (8)$$

At the critical monomer concentration, filaments do not lengthen or shorten:

$$dn/dt = 0 = k^+\bar{c}_1 - k^-_T\bar{a}_1 - k^-_D(1 - \bar{a}_1) \quad (9)$$

$\bar{a}_1$ is the probability that the terminal subunit binds ATP at the critical monomer concentration.

(ii) Reversible Assembly Reaction Followed by a Reversible Conformational Change. Monomers and filament subunits are assumed to occur in two conformations terms "g" and "p". A reaction scheme is depicted in Figure 9. Actin molecules can bind to filament ends and dissociate from filament ends in both conformations. Both monomers and filament subunits can change their conformations reversibly. Filament subunits are assumed to change their conformation independently of the conformation of adjacent subunits. However, the rate constants of assembly and disassembly are assumed to depend on the conformation of actin monomers and filament subunits. ATP hydrolysis is assumed to lag behind polymerization and conformational change. The rate constants and equilibrium constants are defined in Figure 9. The equilibrium constants are correlated to the equilibrium concentrations and rate constants in the following way:

$$K'_{con} = \bar{c}_{1g}/\bar{c}_{1p} \quad (10)$$

$\bar{c}_{1g}$ and $\bar{c}_{1p}$ are the equilibrium concentrations of actin monomers in the g or p conformation, respectively.

$$K_{con} = \frac{1 - \bar{a}}{\bar{a}} = \frac{k^+_{con}}{k^-_{con}} \quad (11)$$

$\bar{a}$ is the equilibrium probability that a filament subunit is in the g conformation.

$$K_{gg} = \frac{c_p\bar{a}^2}{\bar{c}_{1g}c_p\bar{a}} = \frac{\bar{a}}{\bar{c}_{1g}} = \frac{k^+_{gg}}{k^-_{gg}} \quad (12)$$

c_p is the concentration of filament ends.

$$K_{gp} = \frac{\bar{c}_{1g}c_p(1 - \bar{a})}{c_p\bar{a}(1 - \bar{a})} = \frac{\bar{c}_{1g}}{\bar{a}} = \frac{k^-_{gp}}{k^+_{gp}} \quad (13)$$

$$K_{pg} = \frac{c_p(1 - \bar{a})\bar{a}}{\bar{c}_{1p}c_p\bar{a}} = \frac{1 - \bar{a}}{\bar{c}_{1p}} = \frac{k^+_{pg}}{k^-_{pg}} \quad (14)$$

$$K_{pp} = \frac{\bar{c}_{1p}c_p(1 - \bar{a})}{c_p(1 - \bar{a})^2} = \frac{\bar{c}_{1p}}{1 - \bar{a}} = \frac{k^-_{pp}}{k^+_{pp}} \quad (15)$$

The equilibrium constants are not independent. One can demonstrate by appropriate combination of eq 10–15 that the equilibrium concentrations are determined by three independent equilibrium constants, e.g., K_{con}, K'_{con}, and K_{gg}. The other equilibrium constants K_{gp}, K_{pg}, and K_{pp} can be expressed in terms of K_{con}, K'_{con}, and K_{gg}:

$$K_{gp} = K_{gg}^{-1} \quad (16)$$

$$K_{pg} = K_{gg}K_{con}K'_{con} \quad (17)$$

$$K_{pp} = (K_{gg}K_{con}K'_{con})^{-1} \quad (18)$$

The rate of elongation of filaments is given by (Figure 9)

$$dn/dt = c_{1g}a_1k^+_{gg} + c_{1g}(1 - a_1)k^+_{gp} + c_{1p}a_1k^+_{pg} + c_{1p}(1 - a_1)k^+_{pp} - k^-_{gg}a_1a_2 - k^-_{gp}a_1(1 - a_2) - k^-_{pg}(1 - a_1)a_2 - k^-_{pp}(1 - a_1)(1 - a_2) \quad (19)$$

n is the number of filament subunits. c_{1g} and c_{1p} are the concentrations of monomeric actin in the g or p conformation, respectively. a_1 and a_2 are the probabilities that the first or second subunit from the end of a filament is in the g conformation.

The polymerization curves depicted in Figures 2 and 3 show that the rate of growth depends solely on the monomer concentration c_1 ($c_1 = c_{1g} + c_{1p}$). The rate of growth is independent of other conditions (e.g., initial monomer concentration) if the change between the g and p conformation of the monomers is so fast that the g monomers and the p monomers are in equilibrium (eq 19 and 10):

$$c_{1g}/c_{1p} = K'_{con} \quad (20)$$

The probabilities a_1 and a_2 have to be expressed in terms of the rate constants and of the monomer concentration. The values of a_1 and a_2 can be calculated in the following way. If the monomer concentration changes sufficiently slowly, a steady state is established in which the probabilities a_n are determined by the rate of influx of g and p monomers at the filament end and by the rate of conversion of g subunits into p subunits and vice versa:

$$\sum_1^\infty \frac{da_n}{dt} - \frac{dn}{dt}\bar{a} = 0 \quad (21)$$

The second term $(dn/dt)\bar{a}$ compensates for the increasing number of g or p subunits of a growing filament. The probability a_n that the nth subunit from the end of a filament is in the g conformation approaches $\bar{a}$ toward the center because the subunits near the center of a filament were incorporated first and had more time for transitions between the g and p conformations than the terminal subunits. The time derivative of the probability a_n ($n \geq 2$) is given by (Figure 9)

$$da_n/dt = (c_{1g}[a_1k^+_{gg} + (1 - a_1)k^+_{gp}] + c_{1p}[a_1k^+_{pg} + (1 - a_1)k^+_{pp}])[a_{n-1}(1 - a_n) - (1 - a_{n-1})a_n] + [k^-_{gg}a_1a_2 + k^-_{gp}a_1(1 - a_2) + k^-_{pg}(1 - a_1)a_2 + k^-_{pp}(1 - a_1)(1 - a_2)][a_{n+1}(1 - a_n) - (1 - a_{n+1})a_n] - k^+_{con}a_n + k^-_{con}(1 - a_n), \quad n \geq 2 \quad (22)$$

and

$$da_1/dt = c_{1g}(1 - a_1)k^+_{gp} - c_{1p}a_1k^+_{pg} - k^-_{gp}a_1(1 - a_2) + k^-_{pg}(1 - a_1)a_2 - k^+_{con}a_1 + k^-_{con}(1 - a_1) \quad (23)$$

In a steadily growing filament, the probability a_n can be assumed to decay or increase from the terminal to the central subunits in a geometric series:

$$a_n = (a_1 - \bar{a})r^{n-1} - \bar{a} \quad (24)$$

where r is a constant. By combining eq 21 and 24, an equation is obtained that contains a_1 and r. For calculation of a_1 and r, a second equation is necessary. The steady-state approximation for the terminal subunit can be used as an additional equation:

$$da_1/dt = 0 \quad (25)$$

The rate of elongation of actin filaments can be calculated for a given monomer concentration and for a set of rate constants by combining eq 19–25.

The polymerization curves reach the critical monomer concentration $\bar{c}_{1g} + \bar{c}_{1p}$ faster than fitted exponential curves (Figure 4). In a logarithmic representation, the polymerization curves are convex (Figures 5 and 6). In the following section, it will be discussed how the shape of the curves depends on the magnitude of the rate constants. Equation 25 can be modified by combination with eq 11, 13, 14, 16, 17, 20, and 23:

$$k^-_{gp}\left[c_{1g}\frac{1}{K_{gp}}(1 - a_1) - a_1(1 - a_2)\right] - k^-_{pg}\left[c_{1g}\frac{1}{K_{gp}}a_1\frac{1 - \bar{a}}{\bar{a}} - (1 - a_1)a_2\right] = k^+_{con}\frac{a_1 - \bar{a}}{1 - \bar{a}} \quad (26)$$

It follows from eq 26 that $a_1 > a_2 > \bar{a}$ if $k^-_{gp} > k^-_{pg}$ or that $a_1 < a_2 < \bar{a}$ if $k^-_{gp} < k^-_{pg}$. The rate of elongation is given by (eq 12–15 and 20)

$$dn/dt = (c_{1g}/\bar{c}_{1g})[k^-_{gg}a_1\bar{a} + k^-_{gp}(1 - a_1)\bar{a} + k^-_{pg}a_1(1 - \bar{a}) + k^-_{pp}(1 - a_1)(1 - \bar{a})] - k^-_{gg}a_1a_2 - k^-_{gp}a_1(1 - a_2) - k^-_{pg}(1 - a_1)a_2 - k^-_{pp}(1 - a_1)(1 - a_2) = (c_{1g}/\bar{c}_{1g})k^+(a_1,\bar{a}) - k^-(a_1,a_2) \quad (27)$$

where

$$k^+(a_1,\bar{a}) = k^-_{gg}a_1\bar{a} + k^-_{gp}(1 - a_1)\bar{a} + k^-_{pg}a_1(1 - \bar{a}) + k^-_{pp}(1 - a_1)(1 - \bar{a})$$

and

$$k^-(a_1,a_2) = k^-_{gg}a_1a_2 + k^-_{gp}a_1(1 - a_2) + k^-_{pg}(1 - a_1)a_2 + k^-_{pp}(1 - a_1)(1 - a_2)$$

The polymerization curves reach the critical monomer concentration ($\bar{c}_{1g} + \bar{c}_{1p}$) faster than fitted exponential curves if the ratio $k^-(a_1,a_2)/k^+(a_1,\bar{a})$ continuously increases as the monomer concentration approaches the critical concentration. This can be achieved if $a_1 > a_2 > \bar{a}$ ($k^-_{gp} > k^-_{pg}$) and if k^-_{pp} is so great that in eq 27 the contribution of the other terms containing k^-_{gg}, k^-_{gp}, and k^-_{pg} is negligible as compared to $k^-_{pp}(1 - a_1)(1 - \bar{a})$. This can also be achieved if the following conditions apply to the probabilities and rate constants: $a_1 < a_2 < \bar{a}$ ($k^-_{gp} < k^-_{pg}$); $k^-_{gg} > k^-_{gp}$, k^-_{pg}, and k^-_{pp}.

The applicability of the steady-state approximation (eq 21 and 25) was tested by Monte Carlo calculations (Figure 10). The selected set of equilibrium and rate constants was also used for the fit to the experimental data (see next section).

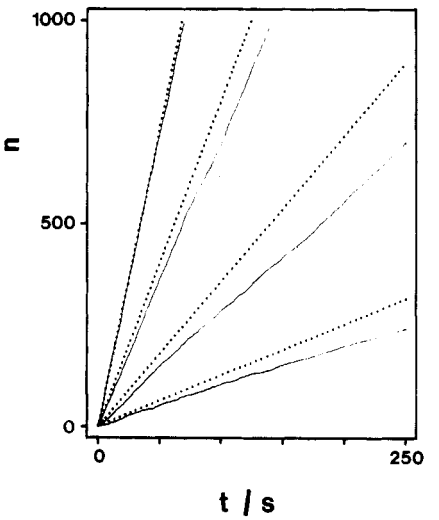

FIGURE 10: Monte Carlo calculation and steady-state approximation of conformational change model: n, number of filament subunits; continuous lines, Monte Carlo calculations (50 times repeated and averaged); dotted lines, steady-state approximations. Monomer concentrations: 1, 2, 5, and 10 μM. $K_{con} = 3$, $k^+_{con} = 0.5\ s^{-1}$, $K'_{con} = 3$, $K_{gg} = 0.555 \times 10^6\ M^{-1}$, $k^-_{gg} = 0.1\ s^{-1}$, $k^-_{gp} = 2\ s^{-1}$, $k^-_{pg} = 0.2\ s^{-1}$, and $k^-_{pp} = 3\ s^{-1}$ (see Figure 5).

Fit of Models to Nucleated Polymerization Curves. Figures 5 and 6 show fits of the two models to the polymerization curves. The number of adjustable parameters (ATP hydrolysis model, k^+, k^-_T, k^-_D, k_P; conformational change model, K_{con}, k^+_{con}, K'_{con}, K_{gg}, k^-_{gg}, k^-_{gp}, k^-_{pg}, k^-_{pp}) is so great that the curves cannot be fitted by a single set of parameters. The calculated curves depicted in Figures 5 and 6 were arbitrarily selected from many well-fitted curves. The ATP hydrolysis model could be fitted if k^-_D was assumed to be greater than k^-_T. The fit to the polymerization curves of ϵ-ATP–actin (Figure 5) was poor if the difference between the rate of dissociation of ϵ-ADP–actin subunits and of ϵ-ATP–actin subunits was within the range of rates reported in the literature (Pollard, 1984). A good fit could be achieved if an ϵ-ADP-bearing subunit is assumed to dissociate very fast as compared to an ϵ-ATP-bearing subunit ($k^-_D/k^-_T > 100$). Good fits of the conformational change model were obtained if k^-_{gp} was assumed to be greater than k^-_{pg} and if k^-_{pp} was assumed to be great as compared to k^-_{gg}, k^-_{gp}, and k^-_{pg}. The observed deviations from linearity could be explained by both models.

Steady-State Phosphate Production. The time courses of steady-state phosphate production by ATP and ϵ-ATP hydrolysis are depicted in Figure 11. The concentration of filament ends was varied. Monomeric actin was polymerized onto different concentrations of polymeric actin. The total actin concentration was kept constant by appropriately adjusting the concentration of monomeric actin added to filaments. The rate of ATP hydrolysis was measured immediately after the final monomer concentration was reached. In this way, possible effects of length redistribution, spontaneous fragmentation, or fragmentation by shear forces were minimized (Oosawa & Asakura, 1975; Wegner & Savko, 1982; Hill, 1983; Grazi & Trombetta, 1985). Figure 11 shows that the steady-state rate of phosphate production does not depend on the concentration of filament ends. The ATP hydrolysis at the ends of actin filaments is negligible compared to the ATP hydrolysis along filaments. One can estimate the steady-state rate of phosphate production expected for the ATP hydrolysis model (Figure 7). In the initial phase of polymerization where the frequency of association reactions prevails over the frequency of dissociation reactions [$k^+c_1 \gg k^-_Ta_1$ +

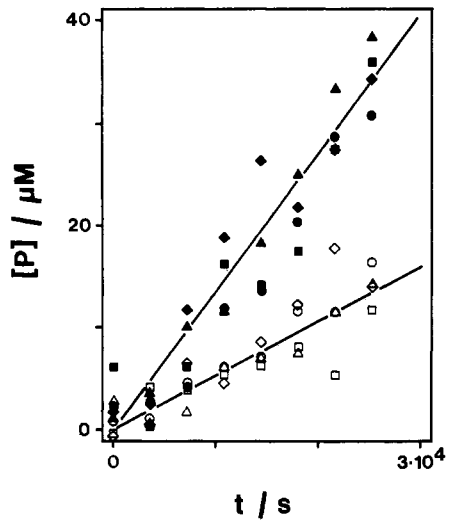

FIGURE 11: Steady-state phosphate production by ϵ-ATP–actin and ATP–actin. Various concentrations of monomeric actin (c_{1i}) were added to various concentrations of polymeric actin (c_{fi}). The phosphate production by hydrolysis of ϵ-ATP or ATP was measured at steady state after the initial polymerization phase. [P], phosphate concentration. ϵ-ATP–actin: (□) c_{1i} = 8 μM, c_{fi} = 2 μM; (○) c_{1i} = 6 μM, c_{fi} = 4 μM; (△) c_{1i} = 4 μM, c_{fi} = 6 μM; (◇) c_{1i} = 2 μM, c_{fi} = 8 μM. The total ϵ-ATP–actin concentration was 10 μM. ATP-actin: (■) c_{1i} = 12 μM, c_{fi} = 3 μM; (●) c_{1i} = 9 μM, c_{fi} = 6 μM; (▲) c_{1i} = 6 μM, c_{fi} = 9 μM; (◆) c_{1i} = 3 μM, c_{fi} = 12 μM. The total ATP–actin concentration was 15 μM.

$k_D^-(1 - a_1)$], the rate of monomer consumption is essentially equal to the association rate ($dc_1/dt \approx -k^+c_1c_p$). At the initial concentration of 16 μM, the monomers are consumed with a rate of about 70 μM/h (Figure 3). At the final critical concentration of 1.4 μM, the rate of association of monomers with filament ends is calculated to be (16/1.4)-fold lower (6 μM/h). In the experiments depicted in Figure 11, the concentration of filament ends was the same or 2-, 3-, or 4-fold higher than that in the experiment depicted in Figure 3. The observed rate of phosphate production is considerably slower than the values expected for the ATP hydrolysis model (1 × 6, 2 × 6, 3 × 6, and 4 × 6 μM/h). An analogous estimation shows that the rates of phosphate production by ϵ-ATP–actin are expected to be 1.8, 3.6, 5.4, and 7.2 μM/h in the four experiments depicted in Figure 11. Also, the steady-state phosphate production by ϵ-ATP–actin cannot be fitted by the ATP hydrolysis model. The conformational change model predicts that the terminal subunits do not contribute to the phosphate production (Figure 9). The measured rates of phosphate production can be explained by the conformational change model.

Discussion

The observed nonlinear increase of the rate of elongation with the monomer concentration was analyzed by two models. In the first model, the ATP hydrolysis by polymeric actin was assumed to be so fast that the terminal subunits of growing filaments bind appreciable amounts of ADP. In the second model, actin monomers and filament subunits were assumed to occur in two conformations. The association and dissociation rates of actin molecules in the two conformations were thought to be different. Monomers and filament subunits had different equilibrium distributions between the two conformations. The nonlinearity could be explained by both models.

The steady-state rate of ATP hydrolysis was found to depend mainly on the concentration of actin filament subunits. A similar result has been reported by Brenner and Korn (1984), who provided evidence that ATP is hydrolyzed by the subunits along Ca–actin filaments. Also, binding of actin molecules to the ends of filaments probably contributes to the ATP hydrolysis as under the experimental conditions actin filaments treadmill (Wegner, 1976; Wegner & Neuhaus, 1981). The incorporation of ATP–actin molecules at the lengthening barbed ends and the production of ADP–actin monomers at the shortening pointed ends result in ATP hydrolysis, the rate of which is proportional to the concentration of filament ends. The contribution of treadmilling to ATP hydrolysis is probably so little that it can hardly be observed apart from hydrolysis by subunits along filaments. Only the rate of phosphate production by ϵ-ATP–actin tends to be faster at higher filament end concentrations (Figure 11). For a good fit of the ATP hydrolysis model to the nucleated polymerization curves, the rate of ATP hydrolysis had to be assumed to be 5 or 2.5 s^{-1} (Figures 5 and 6). This fitted rate is about 100-fold faster than more directly determined values (Pollard & Weeds, 1984; Carlier et al., 1984). Pantaloni et al. (1985b) have proposed that ATP is hydrolyzed at an interface between a cap of a few terminal ATP-containing subunits and the ADP-containing subunits of the core of actin filaments. Also, this model predicts a steady-state rate of ATP hydrolysis that is about equal to the rate of association of monomers with filament ends. These arguments make it unlikely that ATP hydrolysis accounts for the nonlinear correlation between the monomer concentration and the rate of polymerization of lengthening filaments. It is, therefore, obvious to postulate that the assembly reaction of lengthening actin filaments consists of a bimolecular association step that is followed by a conformational change.

We considered also the possibility that the nonlinearity above the critical concentration might be caused by a superimposition of the rates of growth of the barbed and of the pointed ends. The critical monomer concentrations of the two ends are different under the selected experimental conditions. A discontinuity of the rate of elongation at the higher critical concentration of the pointed ends may lead to a nonlinearity above the total critical concentration. Determinations of the rates of elongation and shortening of gelsolin-capped actin filaments showed that the contribution of the pointed ends to the rate of elongation is too little to account for the nonlinearity above the total critical monomer concentration (data not shown).

The conformational change model does not question the interpretation of nonlinearity at the critical monomer concentration as proposed by Carlier et al. (1984). This nonlinearity has been explained by the different composition of lengthening and shortening filaments. Lengthening filaments contain terminal ATP subunits whereas shortening filaments contain terminal ADP subunits. The conformational change model was developed for explanation of the nonlinearity of lengthening filaments above the critical monomer concentration.

Several studies have been reported in which conformational changes of actin have been investigated. Magnesium ions have been found to induce a conformational change of monomeric actin (Frieden, 1982; Cooper et al., 1983). The conformational change requires ATP (Frieden & Patane, 1985). Actin has been reported to change its conformation on transition from the monomeric to the polymeric state (Higashi & Oosawa, 1965). In this study, a shift of the equilibrium distribution of two conformations on polymerization has been proposed. It is an open question whether or not these conformational changes are identical.

Acknowledgments

We thank E. Werres for excellent technical assistance.

Registry No. ATP, 56-65-5; Mg, 7439-95-4.

REFERENCES

Bonder, E. M., Fishkind, D. J., & Mooseker, M. S. (1983) *Cell (Cambridge, Mass.) 34*, 491–501.

Brenner, S. L., & Korn, E. D. (1983) *J. Biol. Chem. 258*, 5013–5020.

Brenner, S. L., & Korn, E. D. (1984) *J. Biol. Chem. 259*, 1441–1446.

Carlier, M.-F., Pantaloni, D., & Korn, E. D. (1984) *J. Biol. Chem. 259*, 9983–9986.

Chen, Y.-D., & Hill, T. L. (1983) *Proc. Natl. Acad. Sci. U.S.A. 80*, 7520–7523.

Cooke, R. (1975) *Biochemistry 14*, 3250–3256.

Cooper, J. A., Buhle, E. L., Walker, S. B., Tsong, T. Y., & Pollard, T. D. (1983) *Biochemistry 22*, 2193–2202.

Detmers, P., Weber, A., Elzinga, M., & Stephens, R. E. (1981) *J. Biol. Chem. 256*, 99–105.

Frieden, C. (1982) *J. Biol. Chem. 257*, 2882–2886.

Frieden, C., & Patane, K. (1985) *Biochemistry 24*, 4192–4196.

Grazi, E., & Trombetta, G. (1985) *Biochem. J. 232*, 297–300.

Grazi, E., Trombetta, G., & Magri, E. (1984) *Biochem. Int. 9*, 669–674.

Higashi, S., & Oosawa, F. (1965) *J. Mol. Biol. 12*, 843–865.

Hill, T. L. (1983) *Biophys. J. 44*, 285–288.

Hill, T. L., & Kirschner, M. W. (1982) *Int. Rev. Cytol. 78*, 1–125.

Hill, T. L., & Carlier, M.-F. (1983) *Proc. Natl. Acad. Sci. U.S.A. 80*, 7234–7238.

Martin, J. B., & Doty, D. M. (1949) *Anal. Chem. 21*, 965–967.

Neidl, C., & Engel, J. (1979) *Eur. J. Biochem. 101*, 163–169.

Oosawa, F., & Kasai, M. (1962) *J. Mol. Biol. 4*, 10–21.

Oosawa, F., & Asakura, S. (1975) *Thermodynamics of the Polymerization of Protein*, pp 51–55, Academic, New York.

Pantaloni, D., Carlier, M.-F., & Korn, E. D. (1985a) *J. Biol. Chem. 260*, 6572–6578.

Pantaloni, D., Hill, T. L., Carlier, M.-F., & Korn, E. D. (1985b) *Proc. Natl. Acad. Sci. U.S.A. 82*, 7207–7211.

Pardee, J. D., & Spudich, J. A. (1982) *J. Cell Biol. 93*, 648–654.

Pollard, T. D. (1983) *Anal. Biochem. 134*, 406–412.

Pollard, T. D. (1984) *J. Cell Biol. 99*, 769–777.

Pollard, T. D., & Mooseker, M. S. (1981) *J. Cell Biol. 88*, 654–659.

Pollard, T. D., & Weeds, A. G. (1984) *FEBS Lett. 170*, 94–98.

Rees, M. K., & Young, M. (1967) *J. Biol. Chem. 242*, 4449–4458.

Rich, S. A., & Estes, J. A. (1976) *J. Mol. Biol. 104*, 777–792.

Rouayrenc, J.-F., & Travers, F. (1981) *Eur. J. Biochem. 116*, 73–77.

Schröer, E., & Wegner, A. (1985) *Eur. J. Biochem. 153*, 515–520.

Secrist, J. A., Barrio, J. R., Leonard, N. L., & Weber, G. (1972) *Biochemistry 11*, 3499–3506.

Seidel, D. T., v. Chak, D., & Weber, H. H. (1967) *Biochim. Biophys. Acta 140*, 93–108.

Wanger, M., & Wegner, A. (1983) *FEBS Lett. 162*, 112–116.

Wegner, A. (1976) *J. Mol. Biol. 108*, 139–150.

Wegner, A. (1982) *J. Mol. Biol. 161*, 607–615.

Wegner, A. (1985) *Nature (London) 313*, 97–98.

Wegner, A., & Neuhaus, J.-M. (1981) *J. Mol. Biol. 153*, 681–693.

Wegner, A., & Savko, P. (1982) *Biochemistry 21*, 1909–1913.